Journal of Organometallic Chemistry 694 (2009) 1185–1188

Contents lists available at ScienceDirect

Journal of Organometallic Chemistry

journal homepage: www.elsevier.com/locate/jorganchem

Synthesis and characterisation of a ruthenocenoyl bioconjugate with the cyclic octapeptide octreotate

Annika Gross, Nils Metzler-Nolte *

Faculty of Chemistry and Biochemistry, University of Bochum, Universitätsstrasse 150, D-44801 Bochum, Germany

ARTICLE INFO

Article history:
Received 2 August 2008
Accepted 29 September 2008
Available online 17 October 2008

Dedicated, in Eb[7], to Professor Dr. Christoph Elschenbroich on the occasion of his 70th birthday

Keywords:
Bioorganometallic chemistry
Bioconjugates
Medicinal organometallic chemistry
Metallocenes
Peptides
Ruthenium compounds

ABSTRACT

The reaction of activated ruthenocene carboxylic acid with the resin-bound peptide octreotate yields, after cleavage and purification by preparative HPLC, the first ruthenocenoyl peptide bioconjugate **1**. Octreotate is a chemically stabilized analogue of somatostatine. It is a cyclic octapeptide with a disulfide bond and has been previously used for molecular diagnostics due to the fact that somatostatine receptors are over-expressed by a variety of cancer cells. Conjugate **1** was obtained in good yield and purified by preparative HPLC to >95% purity as judged by analytical HPLC. It has been identified by HPLC, IR and mass spectrometry (ESI and MALDI-TOF). The peptide's NMR signals are assigned by standard 2D methods. In addition, the ^{1}H NMR spectrum of **1** shows characteristic signals for the metallocene between 5.1 and 4.3 ppm. Compound **1** thus is a new example of tumor-targeted organometallic ruthenium bioconjugates.

1. Introduction

Conjugates of biomolecules with organometallic complexes are receiving increased attention for applications in biosensors, molecular diagnostics, and analytical tools. By far the most frequently used metal complex for biosensor applications is ferrocene (dicyclopentadienyl iron, Cp_2Fe) [1–5]. This is due to the ease of synthesis of functionalized derivatives as well as its favourable electronic properties, in particular the high stability of the +II and +III oxidation states. The electronic structure of the paramagnetic ($S = ½$) +III oxidation state has been studied in detail by EPR spectroscopy [6–8]. Its properties have been compared by Elschenbroich and coworkers to their open-ring analogues and an explanation of the differences has been offered based on electronic structure calculations [9].

Given the abundance of ferrocene bioconjugates, we note with astonishment the almost complete lack of biological applications of other metallocenes with the ferrocene structure. A few cobaltocenium conjugates with peptide nucleic acid oligomers (PNA) [10,11] and peptides [12–15] have been published by our group. Ruthenocene has been mentioned in a few early papers exclusively in the context of radiolabelling with ^{103}Ru [16–19], and more recently labelling of estradiol by ruthenocene was proposed by Jaouen and coworkers [20]. Gmeiner et al. have recently reported ruthenocene derivatives of dopamine receptor ligands which show an increased affinity and specificity for the D4 dopamine receptor subtypes compared to their metal-free congeners [21]. Organometallic Ru(II) arene compounds alone, on the other hand, were investigated by several groups for their anti-proliferative properties, making them promising anti-cancer drug candidates [22–26].

In this work, we report the first ruthenocene peptide bioconjugate, in which ruthenocene carboxylic acid is coupled to the N-terminus of the cyclic octapeptide ocreotate by a peptide bond. Octreotate is an analogue of the naturally occurring peptide somatostatine. Compared to somatostatine, octreotate has a shortened amino acid sequence, shows enhanced stability under biological conditions, and a higher affinity to the somatostatine receptor subtypes 2 [27,28]. Somatostatine receptors (SSTRs) are over-expressed on several tumors and have been successfully targeted for imaging, especially with ^{99m}Tc and ^{111}In (Octreoscan®) [29,30]. The challenge of this work was to establish suitable conditions of solid phase peptide synthesis (SPPS) that will allow the incorporation of a ruthenocene derivative as part of the SPPS cycle, which in the case of octreotate includes a further step for formation of the disulfide bond.

* Corresponding author. Tel.: +49 (0)234 32 28152; fax: +49 (0)234 32 14378.
E-mail address: nils.metzler-nolte@ruhr-uni-bochum.de (N. Metzler-Nolte).

0022-328X/$ - see front matter © 2008 Elsevier B.V. All rights reserved.
doi:10.1016/j.jorganchem.2008.09.071

2. Experimental section

2.1. Materials

Ruthenocene carboxylic acid was synthesized according to literature procedures [31–33]. Chemicals and solvents were used as received from commercial suppliers. Only enantiomerically pure amino acids were used throughout, absolute chirality is given.

2.2. Instrumentation and analytical measurements

A Liberty Microwave Peptide Synthesizer from CEM was used for peptide synthesis. HPLC analysis and purifications were carried out using C18 analytical (Varian Dynamax, 4.5 mm × 250 mm) and C18 semipreparative (Varian Dynamax, 21.4 mm × 250 mm) columns on a customized Varian Prostar Instrument. IR data were collected on a Bruker Tensor 27 with an ATR unit. ESI-MS analyses were performed on a Bruker Esquire 6000 instrument. The matrix-assisted laser desorption/ionization time of flight mass spectrometry (MALDI-TOF) mass spectra were measured on a Bruker Daltonics Autoflex. The experiments were performed in linear mode with positive polarity using sinapinic acid as the matrix. Nuclear magnetic resonance spectra were recorded on a Bruker DRX 600 MHz spectrometer. ^{1}H and ^{13}C chemical shifts are given in ppm and were referenced with the residual solvent resonances relative to tetramethylsilane (TMS). Lyophilization was performed on a Alpha 1-4 LD plus lyophilizator from Christ.

2.3. Synthesis of ruthenocenoyl-octreotate conjugate 1

Fmoc-Octreotate was synthesized on an automated peptide synthesizer by solid phase methods using a 0.25 mmol scale Fmoc-strategy on Fmoc-Thr(^{t}Bu)-Wang resin (0.63 mmol/g, Iris Biotech) generating the C-terminal carboxylic acid after cleavage. The resin-bound peptide sequence was D-Phe-Cys(Acm)-Phe-D-Trp-Lys(Boc)-Thr(tBu)-Cys(Acm)-Thr(tBu)-Wang-resin. Stepwise coupling reactions were performed with enantiomerically pure Fmoc-protected amino acids (IRIS Biotech GmbH or Novabiochem), 1-hydroxybenzotriazole (HOBt), 2-(1H-benzotriazol-1-yl)-1,3,3-tetramethyl-uroniumtetrafluoroborate (TBTU), diisopropyl-ethylamine (DIPEA), (4:4:4:6 equiv., cystein coupling: 50 °C, 0 W, 120 s, followed by 50 °C, 25 W for 240 s. Other amino acids were coupled using: 75 °C, 24 W, 300 s). 2-fold N-terminal deprotection of the Fmoc group was performed using 20% piperidine solution in DMF (first cycle: 75 °C, 35 W, 30 s; second cycle 75 °C, 50 W, 180 s). A total of 0.055 mmol of the resin-bound side-chain protected Fmoc-Octreotate was transferred into a batch reactor, followed by cyclization at room temperature with a 2-fold molar excess of thallium(III)trifluoroacetate ($Tl(TFA)_3$) in DMF for 1 h [34]. After washing with DMF, ruthenocene carboxylic acid (0.22 mmol, 0.0605 g) was coupled using O-(7-Azabenzotriazol-1-yl)-*N*,*N*,*N*′,*N*′-tetramethyluronium-hexafluorophosphate (HATU) (0.22 mmol, 0.084 g), 56.4 μL DIPEA (4:4:6) in 500 μL NMP for 3 h. The completeness of ruthenocene carboxylic acid coupling was determined by Kaiser's test [35]. The resin was washed with DMF and DCM, shrinked with MeOH and dried under vacuum for 30 min. Finally, cleavage of the bioconjugate from the resin was performed with TFA/phenol/triisopropylsilane (TIS) (2 mL, 85:10:5) for 2 h at room temperature. The resin was filtered and washed with 0.5 mL TFA. Addition of cold diethyl ether yielded a beige precipitate, which was washed repeatedly with diethyl ether. The product was dissolved in acetonitrile/water, filtered and lyophilized. The crude yield was 75% (0.053 g), see Fig. 1. The bioconjugate was purified by RP-HPLC using a gradient of acetonitrile/water containing 0.1% TFA (60 min, 4 mL/min). The fractions containing the conjugate were collected and lyophilized. The purity of the conjugate was 95% as determined by analytical HPLC (Fig. 2). IR (neat, ATR): 3293 (br, ν_{NH}), 1643 (s, $\nu_{CO(1)}$), 1526 (m, $\nu_{CO(2)}$). MALDI-TOF MS: *m/z* 1289.9 $(M+H)^+$; ESI-MS (pos.): 1291.22 $(M+3H)^+$, Calc. for $C_{60}H_{70}N_{10}O_{12}RuS_2$: 1288.4; ^{1}H NMR (DMSO-d_6, 600 MHz): δ 10.77 ($1H_{\varepsilon 1,\ Trp4}$), 8.88 ($1H_{NH,\ Cys2}$), 8.74 ($1H_{NH,\ Trp4}$), 8.52 ($1H_{NH,\ Phe3}$), 8.46 ($1H_{NH,\ Cys7}$), 8.42 ($1H_{NH,\ Lys5}$), 8.31 ($1H_{NH,\ Thr8}$), 7.64 ($3H_{\zeta,\ Lys5}$), 7.57 ($1H_{NH,\ Thr6}$), 7.48 ($1H_{NH,\ Phe1}$), 7.46 ($1H_{\varepsilon 3,\ Trp4}$), 7.35 ($2H_{\delta,\ Phe1}$), 7.34 ($1H_{\zeta 2,\ Trp4}$), 7.28 ($2H_{\varepsilon,\ Phe1}$), 7.18 ($1H_{\zeta,\ Phe1}$), 7.12 (3H, $2H_{\varepsilon,\ Phe3}$, $1H_{\zeta,\ Phe3}$), 7.07 ($1H_{\eta 2,\ Trp4}$), 7.04 ($2H_{\delta,\ Phe3}$), 6.99 ($1H_{\zeta 3,\ Trp4}$), 6.97 ($1H_{\delta 1,\ Trp4}$), 5.32 ($1H_{\alpha,\ Cys7}$), 5.27 ($1H_{\alpha,\ Cys2}$), 5.14 ($1H_{Cp2}$), 5.06 ($1H_{Cp5}$), 4.94 ($1H_{\alpha,\ Phe1}$), 4.82 ($1H_{\gamma 1,\ Thr6}$), 4.63 (3H, $2H_{Cp3,4}$, $1H_{\alpha,\ Phe3}$), 4.55 ($1H_{\alpha,\ Thr6}$), 4.34 (6H, $1H_{\beta,\ Thr8}$, $2H_{Cp'}$), 4.26 (2H, $1H_{\alpha,\ Thr8}$, $1H_{\alpha,\ Trp4}$), 4.12 ($1H_{\gamma 1,\ Thr8}$), 4.03 ($1H_{\alpha,\ Lys5}$), 3.97 ($1H_{\beta,\ Thr6}$), 3.15 ($1H_{\beta 2,\ Phe1}$), 2.98 ($1H_{\beta 2,\ Trp4}$), 2.92 ($1H_{\beta 3,\ Phe1}$), 2.87 (3H, $H_{\beta 2,\ Cys2}$, $H_{\beta 2,\ Cys7}$, $H_{\beta 2,\ Phe3}$), 2.85 ($1H_{\beta 3,\ Phe3}$), 2,82 (2H, $H_{\beta 3,\ Cys2}$, $H_{\beta 3,\ Cys7}$), 2.75 ($1H_{\beta 3,\ Trp4}$), 2.61 ($2H_{\varepsilon,\ Lys5}$), 1.75 ($1H_{\beta 2,\ Lys5}$), 1.32 (3H, $1H_{\beta 3,\ Lys5}$, $2H_{\delta,\ Lys5}$), 1.20 ($3H_{\gamma 2,\ Thr8}$), 1.06 ($3H_{\gamma 2,\ Thr6}$), 0.83 ($2H_{\gamma,\ Lys5}$). ^{13}C NMR (DMSO-d_6, 150 MHz): δ 172.7 (CO, $_{Phe1}$), 171.8 (CO, $_{Trp4}$), 171.6 (CO, $_{Thr8}$), 170.8 (CO, $_{Lys5}$), 170.3 (CO, $_{Phe3}$), 170.0 (CO, $_{Thr6}$), 169.6 (CO, $_{Cys7}$), 168.6 (CO, $_{Cys2}$), 167.1 (CO, Cp), 138.0 ($C_{\gamma,\ Phe1}$), 136.4 ($C_{\gamma,\ Phe3}$), 135.8 ($C_{\varepsilon 2,\ Trp4}$), 129.0 ($C_{\delta,\ Phe1}$), 128.6 ($C_{\delta,\ Phe3}$), 127.7 ($C_{\varepsilon,\ Phe1}$), 127.6 ($C_{\varepsilon,\ Phe3}$), 126.9 ($C_{\delta 2,\ Trp4}$), 126.0 ($C_{\zeta,\ Phe1}$), 125.9 ($C_{\zeta,\ Phe3}$), 123.3 ($C_{\delta 1,\ Trp4}$), 120.6 ($C_{\eta 2,\ Trp4}$), 117.9 ($C_{\zeta 3,\ Trp4}$), 117.8 ($C_{\varepsilon 3,\ Trp4}$), 111.0 ($C_{\zeta 2,\ Trp4}$),

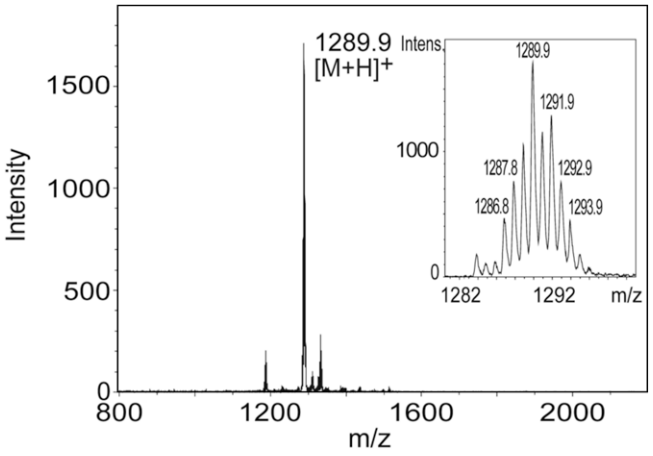

Fig. 1. MALDI-TOF of the crude ruthenocenoyl-octreotate **1**. The inset shows the experimentally observed isotope pattern of the $[M+H]^+$ peak.

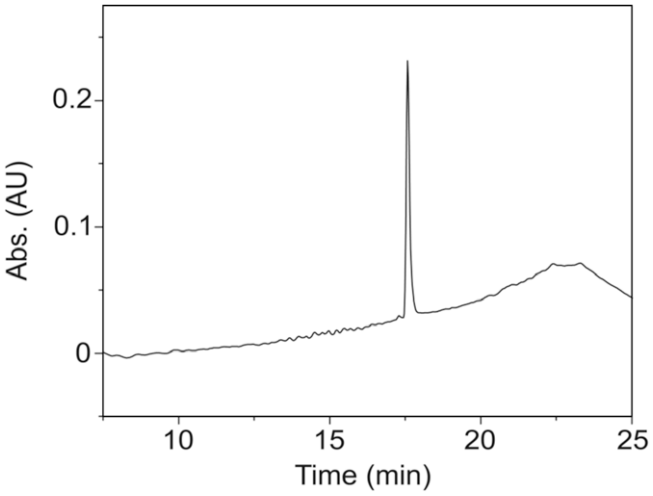

Fig. 2. HPLC trace (220 nm) of the purified ruthenocenoyl-octreotate **1**.